A cell chip for sequential imaging of individual non-adherent live cells reveals transients and oscillations†

Yael S. Schiffenbauer,‡[a] Yael Kalma,‡[a] Ella Trubniykov,[a] Orit Gal-Garber,[b] Lilach Weisz,[a] Asaf Halamish,[a] Michael Sister[a] and Gideon Berke*[b]

Received 10th March 2009, Accepted 29th June 2009
First published as an Advance Article on the web 15th July 2009
DOI: 10.1039/b904778f

Advances in molecular cell biology, medical research, and drug development are driving a growing need for technologies that enable imaging the dynamics of molecular and physiological processes simultaneously in numerous non-adherent living cells. Here we describe a platform technology and software – the CKChip system – that enables continuous, fluorescence-based imaging of thousands of individual living cells, each held at a given position ("address") on the chip. The system allows for sequential monitoring, manipulation and kinetic analyses of the effects of drugs, biological response modifiers and gene expression in both adherent and non-adherent cells held on the chip. Here we present four specific applications that demonstrate the utility of the system including monitoring kinetics of reactive oxygen species generation, assessing the intracellular enzymatic activity, measuring calcium flux and the dynamics of target cell killing induced by conjugated cytotoxic T-lymphocytes. We found large variations among individual cells in the overall amplitude of their response to stimuli, as well as in kinetic parameters such as time of onset, initial rate and decay of the response, and frequency and amplitude of oscillations. These variations probably reflect the heterogeneity of even cloned cell populations that would have gone undetected in bulk cell measurements. We demonstrate the utility of the system in providing kinetic parameters of complex cellular processes such as Ca^{++} influx, transients and oscillations in numerous individual cells. The CKChip opens up new opportunities in cell-based research, in particular for acquiring fluorescence-based, kinetic data from multiple, individual non-adherent cells.

Introduction

Live cell-based assays have become common tools in many fields of biological research and medicine, providing valuable tools in drug discovery and testing. These kinds of assays provide an authentic representation of cell behavior as opposed to working with fixed cells and cell-based chemical assays. Yet, cells may differ from each other in their genetic, biochemical and physiological properties.[1] Hence, the importance of examining individual cells has become increasingly appreciated, since population-based information provides averages that may conceal extreme (either low or high) behavior of cells. The latter could markedly influence averages, possibly yielding false positive or negative results. Moreover, since cellular processes are dynamic, investigating how individual cells function over time allows a better appreciation of physiological and patho-physiological cellular processes. Flow cytometry offers high-throughput, multi-parametric analysis of the physical and/or molecular characteristics of numerous individual cells as they flow through an optical and/or electronic detection apparatus. Yet, it has several shortcomings because it does not enable monitoring individual cells of interest repeatedly, over time, and still requires a relatively large cell sample. Unlike flow cytometry, microscope-based cytometers provide visual information about both cell morphology and spatial distribution of fluorescence within individual cells and are well suited for observing cellular properties as a function of time. Yet, microscopic high content analysis of cellular responses have thus far been limited mainly to adherent cells; relatively little high-content analysis has been done with live non-adherent blood or bone marrow cells, either normal or malignant, and the kinetics of their responses to stimuli have rarely been addressed at the single-cell level because of lack of suitable imaging platforms. Even the most sophisticated microscopic platforms and software, which combine fully automated high throughput and high-content analysis, do not enable kinetic measurements of the same individual, non-adherent cells over extended periods of time. At the same time, the value of research involving non-adherent cell lines and primary cells including normal and malignant blood cells, as well as tumor cell aspirates is undisputed and increasing. To overcome these limitations, different cell array techniques that confine non-adherent cells to particular locations have been developed. Many different approaches have been applied in these arrays including mechanical, electrical, optical and chemical means.[2,3] These techniques include polydimethylsiloxane (PDMS)-based microfluidic devices;[4] passive confinement of cells on etched

[a]*Cell Kinetics, Lod, Israel*
[b]*Department of Immunology, The Weizmann Institute of Science, Rehovot, 76100, Israel. E-mail: Gideon.berke@weizmann.ac.il; Fax: 972-8-9342779; Tel: 972-8-9343975*

† Electronic supplementary information (ESI) available: High resolution images and movie 1 (calcium oscillations). See DOI: 10.1039/b904778f
‡ Equal contribution

glass,[5] lithographed polystyrene,[6] photolithographed SU-8[7] or PDMS[8] microarrays. Other techniques are based on dielectrophoretic[9] or hydrodynamic[10] cell trapping. Most of these techniques do not allow simultaneous monitoring and analysis of thousands of cells over time or require additional dedicated scanners. The CKChip reported here enables capture, and monitoring of up to 10,000 adherent or non-adherent living cells, each held in a micron-sized well. The technology allows for their repeated monitoring and manipulation over extended periods of time thus enabling acquisition of important kinetic information about cellular responses to stimuli. Cells remain functional in their designated "addresses" (micro-wells) on the chip, available for treatment (*e.g.* with drugs, antibodies, and cytokines), as well as cell-based fluorescence imaging on virtually any upright or inverted fluorescence microscope equipped with a digital camera. Acquired images are automatically analyzed by a user friendly, dedicated imaging software – WELLS. The CKChip has a particular advantage in assessing drug effects and responses of non-adherent cells, such as from the blood, bone marrow, stem cells, leukemia, and lymphoma, which are difficult to monitor over time by either flow-cytometry or standard microscopy.

Experimental

The CKChip

The CKChip is composed of the cell carrier, an array of up to 10,000 micron-sized conical wells, mounted on a plastic array holder (Fig. 1). The holder is made by injection molding of biocompatible plastic consisting of a buffer chamber connected to the cell array on top, which is covered with a cover glass, and sealed by a silicon plug. A washing niche allows introduction of cells, sequential addition of reagents and repeated washings by capillary forces created under the cover glass. Excess and waste fluid is collected in the two reservoirs on the side (Fig. 1).

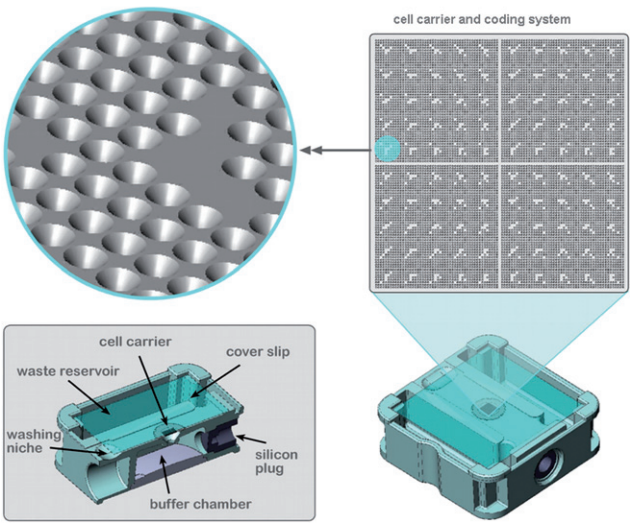

Fig. 1 The CKChip. The CKChip is composed of the cell carrier, an array of micron-sized conical wells mounted on a plastic chip holder. The center of the holder consists of a buffer chamber connected to the array on top and sealed off by a silicon plug on the side. On top of the holder, next to the cell carrier, a washing niche allows introduction of cells, sequential addition of reagents, washings. Waste fluid is collected in two reservoirs on the side. The cell carrier consists of an array of 10,000 conical holes of 10–18 μm upper diameter, 3–5 μm lower diameter, 12–15 μm depth and 20 μm inter-well (pitch) distance and an embedded coding system illustrated and enlarged in the upper panels.

The cell carrier and its coding system

The 2 × 2 mm cell array consists of 10,000 conical holes; 10–18 μm upper diameter, 3–5 μm lower diameters, 12–15 μm depth and 20 μm inter-well (pitch) distance arranged in 4 quarters (Fig. 1). The coding system embedded in the array consists of 25 distinct coding patterns for each quarter, created by blocking 6 specific wells during the manufacturing process through which light is not transmitted. Five of the blocked wells are used to map the exact location in the corresponding row and column and one additional blocked well is used to assign the quarter (upper left, upper right, lower left, lower right) (Fig. 2). The coding system enables manual or computer-guided revisiting of any cell of interest, even after the CKChip has been removed from the microscope stage, returned for additional imaging. Selected cells of interest, or groups of cells, can be continuously and simultaneously tracked, measured, manipulated and analyzed a number of times, with their identities verified by their specific addresses on the grid.

Manufacturing process of the cell array

The cell array is made of nickel by electroforming, a highly specialized process of metal part fabrication using electrodeposition. Briefly, a nickel plate is coated with a photoresist material and exposed to light through a dedicated mask resulting in polymerization of specified locations only. The remaining non-polymerized photoresist is removed and electroforming is performed, the nickel plate acts as the cathode. Nickel starts to build up in the conductive areas of the cathode, in between the photoresist. At the end of the process, the grid formed is separated from the nickel plate, coated with silicon nitride and assembled onto the plastic holder (Fig. 3).

Cell loading, washing, and staining

The chamber of the chip is filled with medium through the filling hole using a micropipette (900 μl). The filled chamber is then sealed-off with a silicon plug. To load cells on the array, a mild positive pressure (1–3 millibars) is created in the buffer chamber by pressing on the silicon plug. A drop containing cells (the concentration depends on the cell type) is then applied to the washing niche. Releasing the pressure applied to the silicon plug, results in siphoning and trapping of cells inside the micro-wells – one cell per well. Unsettled cells are then flushed away by a buffer solution applied under the cover slip through the washing niche. Settled cells withstand exchange of solutions and retain their locations. Depending on the cell type, most non-adherent cells are retained in their original positions for up to 24 hours.

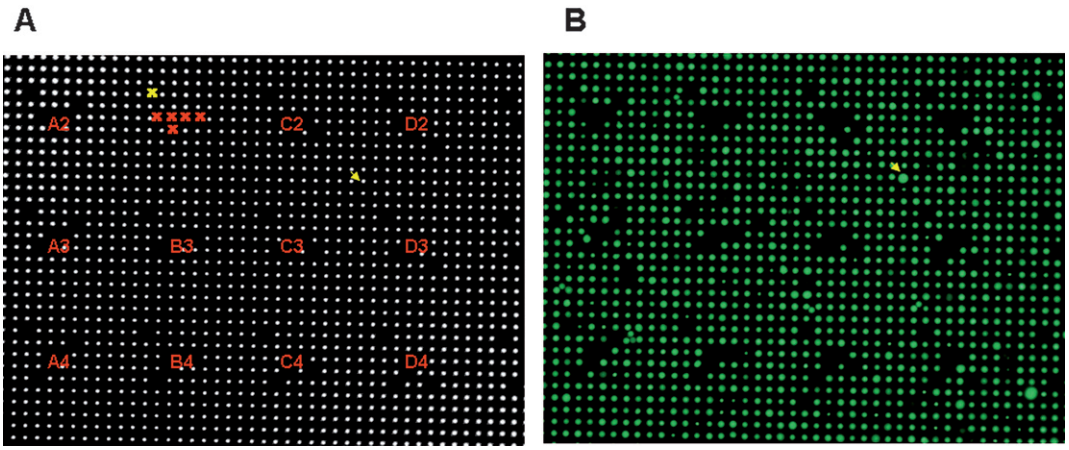

Fig. 2 Transmitted light image of the coding system and the corresponding fluorescent image. The transmitted light image (A) and the corresponding fluorescent image (B) (×10 magnification) of a field of view in the upper left quadrant of the chip are shown. The coding system consists of 25 distinct patterns generated by the blockage of 6 specific wells appearing dark in the transmitted light image and is used to provide a specific address to the cells in wells. Five of the blocked wells assign the code location (red **X**) and one additional blocked well assigns the corresponding quarter (yellow **X**). A selected cell located in well #1930 is denoted by the yellow arrow.

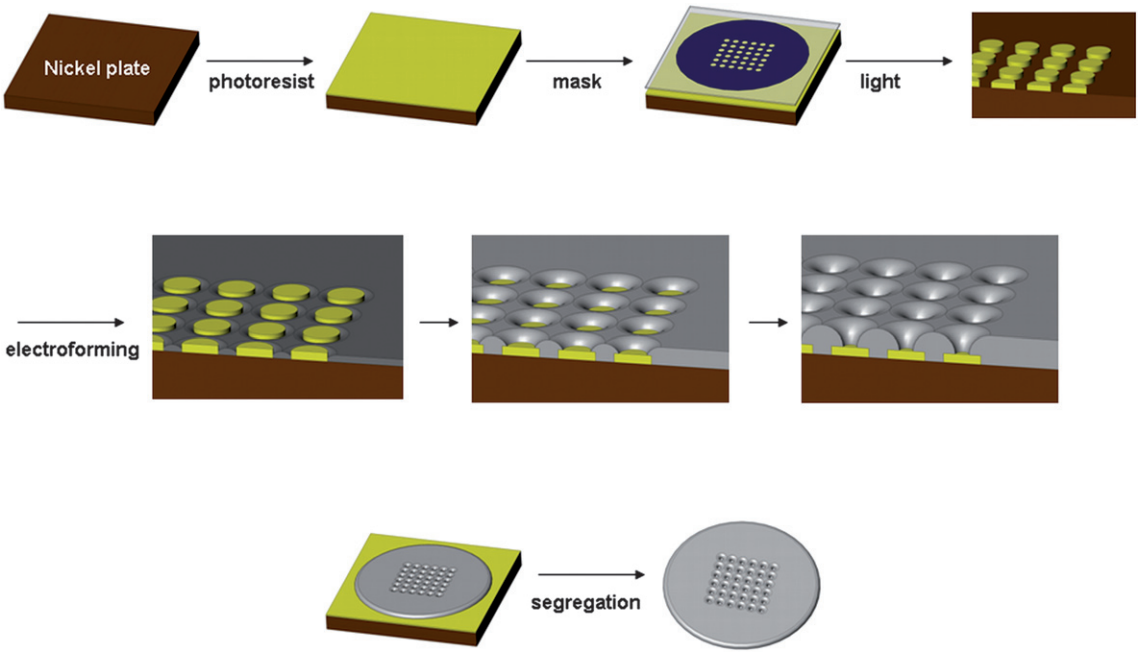

Fig. 3 Manufacturing process of the cell array. A nickel plate is coated with a photoresist material and exposed to light through a dedicated mask resulting in the polymerization of specified locations only. The remaining non-polymerized photoresist is removed and electroforming is performed, the nickel plate acting as the cathode. Nickel starts to build up in the conductive areas of the cathode, in between the photoresist. At the end of the process, the grid formed is separated from the nickel plate.

Imaging

Fluorescently-labeled cells on the CKChip are monitored by either an upright or inverted fluorescence microscope. Fluorescence emanating from the cells is observed with an appropriate set of filters, then photographed by a digital camera for further analysis. The code of the same field of view is observed and photographed using bright field illumination. The built-in code enables revisiting the same cells after removing the sample from the microscope stage.

Image analysis with WELLS software

WELLS is a dedicated software package designed to automatically quantify the fluorescence emanating from individual cells arranged on the chip over time. To this end, the fluorescent and corresponding bright field images collected from different fields of the chip at different time points are loaded into WELLS. WELLS algorithm uses the bright field image, resulting from the transmitted light passing through the chip's micro wells, to identify well locations. Blocked wells, through which light is not transmitted,

generate the coding system allowing designating a specific address (index) to each well/cell in a well. When bright field images are superimposed on the corresponding fluorescent images, the specific address of each cell in all images can be determined (Fig. 2). WELLS software default algorithm was designed to read fluorescence emanating from the area of the well only. When more than one cell in a well or cells out of well are detected, they are excluded from the binary image and thus from the calculations. In the event cell-cell interactions are studied, WELLS software employs a dedicated algorithm that allows to measure more than one cell per well. Conventional image analysis algorithms and noise reduction filters are applied prior to calculating the different fluorescence-based parameters resulting in the quantification of the average and total intensity, the area, perimeter and axial ratio of each cell in the field of view for every time point monitored. Further analysis enables one to discern the kinetic behavior of cells of interest.

Cell culture and mice

Leukemia EL4 of C57BL/6 mice and Jurkat human T leukemia lymphoblasts were grown in RPMI supplemented with 10% fetal calf serum, 1 mM sodium pyruvate, 2 mM glutamine, 100 u/ml penicillin, 0.1 mg/ml neomycin, 0.1 mg/ml streptomycin, 0.1% MEM-Eagle amino acid solution, and 0.05 mM β-mercaptoethanol. Rat Basophilic Leukemia (RBL-2H3, kindly provided by Dr. Ehud Razin, Department of Biochemistry, Hebrew University Medical School, Jerusalem, Israel) were grown without β-mercaptoethanol. H1299 human lung carcinoma cells were grown in DMEM supplemented with 10% fetal calf serum, 2 mM glutamine, 100 u/ml penicillin, 0.0125 u/ml nystatin and 0.1 mg/ml streptomycin. BALB/c mice were acquired from the Weizmann Institute of Science where all animal work was conducted and approved by the Institute Animal Committee.

Microscopy and flow cytometry

Imaging of cell fluorescence was performed on a Nikon 80i fluorescent microscope equipped with a Nikon DS-Fi1 digital camera and a FITC (EX 465–495, DM 505, BA 515–555), TRITC (EX 540/25, DM 565, BA 605–655) and DAPI (EX 340–380, DM 400, BA 435–485) filter blocks. T cell-tumor conjugates were imaged on a Zeiss Axioscop fluorescent microscope equipped with DAPI and FITC filter blocks and a Hamamatsu Photonics C4742-80-12AB digital camera. Calcium flux experiments were performed on a Delta Vision RT Olympus 1x71 system (Works software) equipped with a Photometrics Cool Snap HQ digital camera. Flow cytometry experiments were performed on a Beckman Coulter Cytomics FC 500 system.

Reagents and fluorescent probes

The Image-iT-LIVE reactive oxygen species (ROS) detection kit was purchased from Molecular Probes, consisting of the fluorogenic marker of ROS in live cells 5-(and 6)-carboxy-2′,7′-dichlorodihydrofluorescein diacetate (carboxy-H_2DCFDA), the common ROS inducer tert-butyl hydroperoxide (TBHP) and the cell-permeant nuclear stain Hoechst 33342. Fluo-4, the cell-permeant acetoxymethyl ester (AM) for intracellular calcium measurements, and CellTracker orange for the conjugate assay were purchased from Molecular Probes. IgE anti-DNP (dinitrophenol) monoclonal antibody, DNP-BSA, Hank's Balanced Salt Solution (HBSS buffer) for calcium measurements, calcein for conjugate assay and fluorescein di-acetate (FDA) for enzymatic activity measurements were purchased from Sigma.

Results

Dynamic measurements of multiple individual cells

Here we present four applications that demonstrate the utility of the system in providing kinetic parameters of multiple individual cellular responses:

Kinetics of reactive oxygen species (ROS) generation

ROS are highly reactive small molecules formed at a controlled rate as natural by-products of oxygen metabolism. Under conditions of oxidative stress, ROS production increases, causing alterations in membrane lipids, proteins, and nucleic acids. We employed the CKChip to monitor the kinetics of ROS generation in numerous individual adherent H1299 human lung adenocarcinoma cells following induction of oxidative stress. Cells were loaded on the CKChip and stained with 5-(and 6)-carboxy-2′,7′-dichlorodihydrofluorescein diacetate (carboxy-H_2DCFDA), a fluorogenic indicator of ROS. They were then washed and imaged using a Nikon 80i fluorescent microscope equipped with a FITC filter block and then treated with tert-butyl hydroperoxide (TBHP, 100 μM), a common inducer of ROS. The kinetics of ROS generation in individual cells was followed over time for up to 2 hours (Fig. 4). Images were analyzed and quantified by WELLS dedicated software.

Quantification of the fluorescence emanating from thousands of individual cells over time (reflecting the kinetics of ROS production) revealed a high degree of heterogeneity among a seemingly homogeneous cell population. A rise in ROS levels was detected in most cells starting one hour after treatment with TBHP, but single-cell analysis revealed considerable variations in ROS kinetics among individual cells.

Monitoring intracellular enzymatic activity

Esterases are hydrolytic enzymes that split esters into an acid and an alcohol. Numerous esterases exist that differ in their substrate specificity, protein structure and biological function. One approach for evaluating intracellular esterase activity involves using fluorescein esters, which are cell permeable, non-polar, non-fluorescent compounds that are rapidly hydrolyzed by acetyl esterases to generate fluorescein, a charged fluorescent compound retained by living cells.[11] Since intracellular esterase activity is required to generate the fluorescent product whose retention requires membrane integrity, fluorescein esters are also used for cell viability and membrane permeability assays. Here we used the CKChip to measure the kinetics of intracellular esterase activity as indicated by cleavage of its substrate, fluorescein di-acetate (FDA), and determined how esterase activity varies within a population of cells. For this purpose Jurkat cells were loaded on the CKChip and exposed to 0.12 μM FDA. Images of a thousand cells were acquired every few seconds over 10 minutes and analyzed using WELLS dedicated software. Although esterase activity in all live cells increased over time, up to a 10-fold variation between individual cells was observed (Fig. 5).

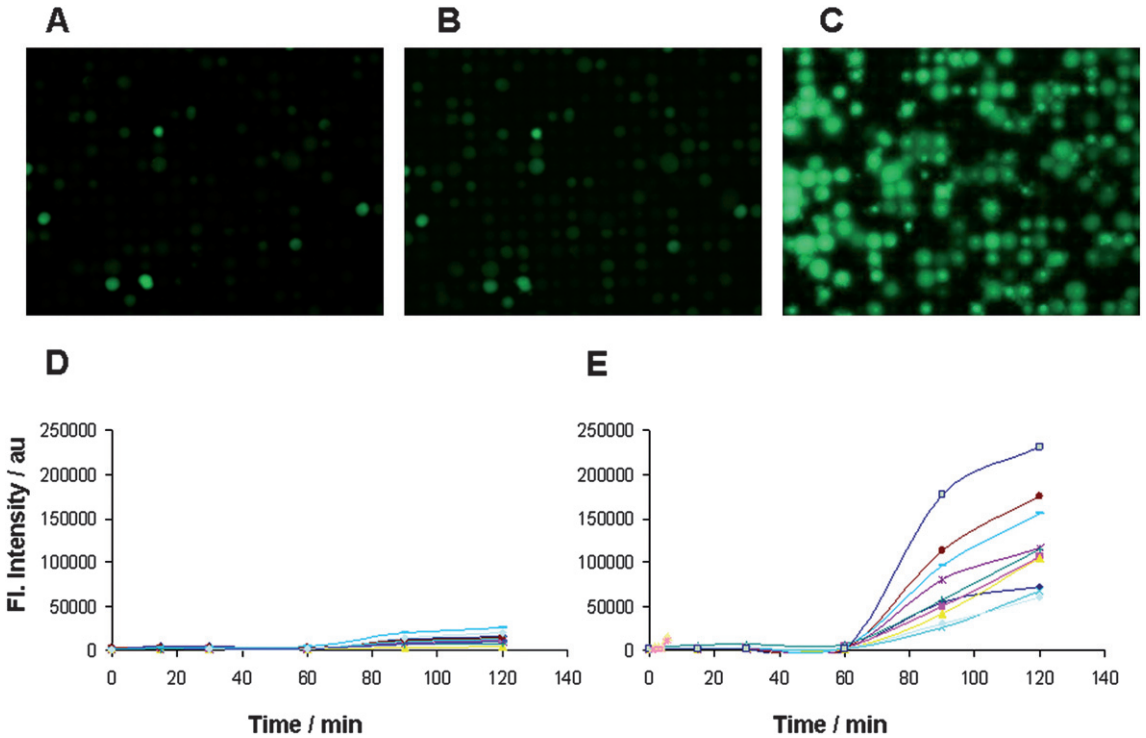

Fig. 4 ROS generation in H1299 cells exposed to oxidative stress. H1299 cells were mounted on the CKChip, stained with carboxy-H2DCFDA, and imaged using a Nikon 80i microscope (A). Thereafter, cells were treated with tert-butyl hydroperoxide (TBHP; 100 μM) and imaged over time for up to 2 hours (B and C after 30 and 120 minutes, respectively). Fluorescence intensity changes over time, correlative with kinetics of ROS generation, are shown for a few typical untreated (D) and TBHP-treated (E) cells.

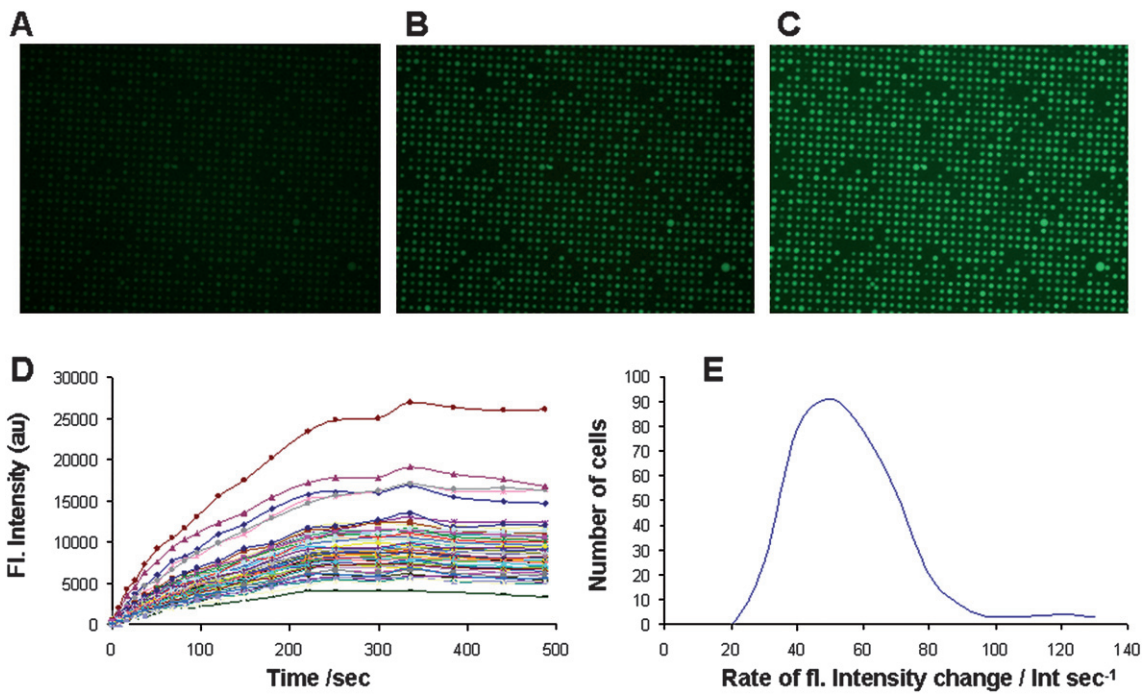

Fig. 5 Kinetics of acetyl esterase activity. Jurkat cells were loaded on the CKChip and exposed to FDA, 0.12 μM, (Sigma). Representative images taken 8 (A), 68 (B) and 500 (C) seconds following FDA addition are shown. The fluorescence intensity of many individual cells over 8 minutes after FDA addition is shown (D). The initial rate of fluorescence increase over the first 2 minutes after FDA addition was calculated for each cell and the distribution of these rates is depicted (E).

Measurement of calcium fluxes and oscillations in numerous, individual cells upon stimulation with antigen

Calcium ions (Ca^{++}) function as a universal second messenger in virtually all eukaryotic cells, playing a vital role in cellular responses to stimuli, mediating various physiological processes.[12] Here we demonstrate the utility of the CKChip system in monitoring the kinetics of calcium fluxes and oscillations in RBL-2H3 cells sensitized with anti-DNP IgE monoclonal antibody and stimulated with DNP-BSA.

RBL-2H3 cells pre-sensitized for 24 hours with a DNP-specific IgE antibody were suspended in HBSS (3×10^6 cells/mL) supplemented with 10 mM HEPES and glucose. Cells were loaded on the CKChip and labeled with the cell-permeable calcium indicator Fluo-4, AM (2 μM) for 20 min at 37 °C. Fluo-4, AM is a visible-light Ca^{++} indicator, which upon binding Ca^{++} ions, undergoes an increase in fluorescence emitted at 525 nanometers when excited at 488 nanometers. Cells were then washed and kept at RT for 15 minutes. While on the chip, cells were stimulated with the corresponding antigen DNP-BSA (100 ng/ml) in a Ca^{++} buffer (HBSS supplemented with 10 mM HEPES, BSA, $MgCl_2$ and 1.8 mM $CaCl_2$) and sequential images were taken every 2.5 seconds for 8 minutes before and after the addition of stimulant (Fig. 6A–C). Cells stimulated in calcium-deficient buffer served as controls (data not shown). The average effect induced by DNP-BSA was a transient increase in Ca^{++}, peaking after 40 seconds, followed by a slow progressive decline. Fast oscillations in intracellular Ca^{++} were observed in most responding cells (Fig. 6D and movie 1 in supplementary material†). Images analyzed by WELLS revealed considerable variability in the response of individual cells, including variability in the frequency and amplitude of oscillations (Fig. 6D). The distinctive oscillatory effect exhibited by the numerous individual cells was lost upon averaging the examined population (Fig. 6E). In parallel, Ca^{++} levels were monitored on a Cytomics FC 500 Beckman-Coulter flow cytometer at different time points before and after DNP-BSA stimulation. The results obtained by microscopic imaging on the CKChip and by flow cytometry showed a similar increase over time (Fig. 6F). Yet the CKChip provided additional information revealing oscillating behavior of intracellular Ca^{++} over time in single cells, which went undetectable in flow cytometry.

Dynamics of target cell killing by cytotoxic T-lymphocytes (CTLs)

A multi-cellular (usually bi-cellular) cluster comprising a T (or B or NK) lymphocyte bound to a cognate antigen-presenting cell is termed a conjugate.[13,14] Conjugate formation between activated CD8 cytotoxic T lymphocytes (CTL) and antigen-presenting target cells is the first event in a multi-step process that ultimately leads to destruction of the bound target cell; the initially bound effector CTL ultimately detaches and is able to start a fresh round

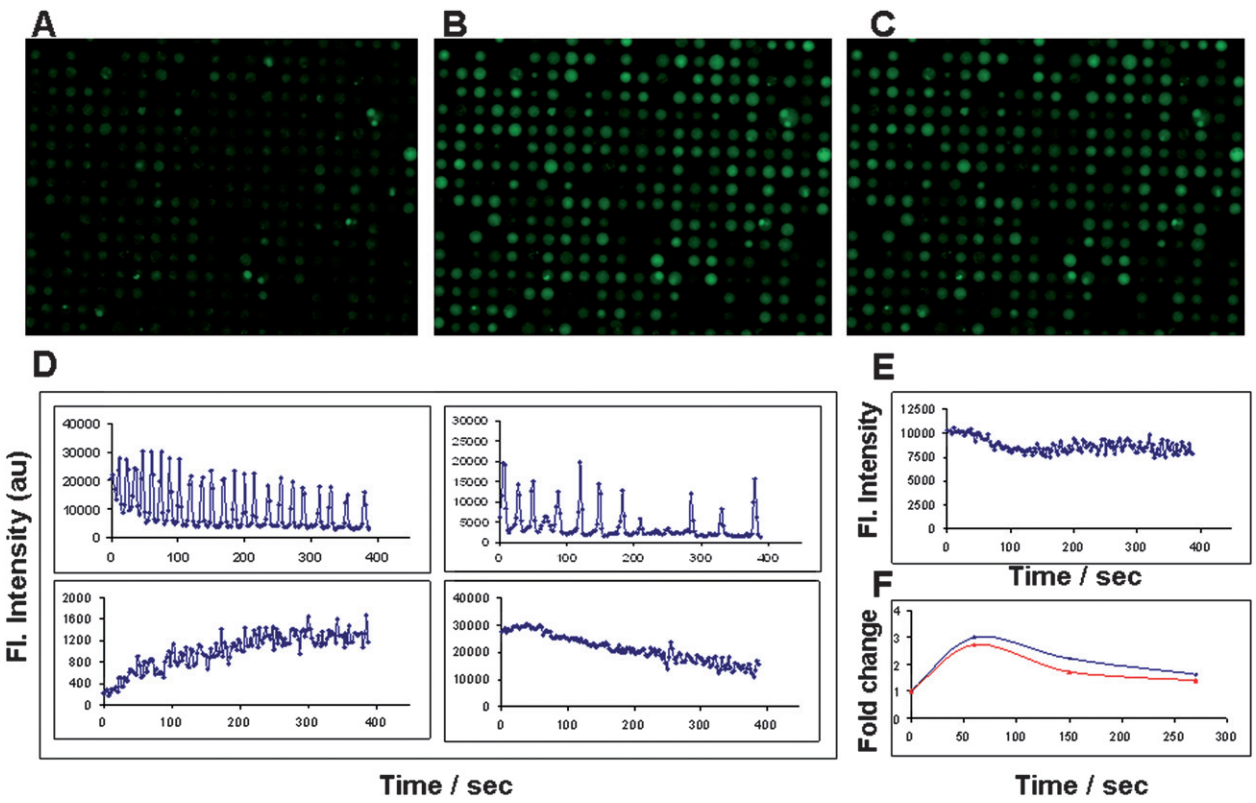

Fig. 6 Detection of calcium transients and oscillations in IgE-sensitized RBL-2H3 cells upon stimulation with DNP-BSA. RBL-2H3 cells were sensitized for 24 hours with a DNP-specific IgE antibody, loaded on the CKChip and labeled with Fluo-4, AM. DNP-BSA (antigen, 100 ng/ml) was added in Ca^{++}-containing buffer and images were taken every 2.5 seconds over 8 minutes before and after addition of DNP-BSA. Representative images (x20 magnification) collected at 0 (A), 1 (B), and 3 (C) minutes after adding DNP-BSA are shown. Representative results collected after stimulation from individual cells (D) and from the average of the whole population (E) are presented. Average fold changes in fluorescence intensity at different time points were determined by both CKChip (blue) and FACS (red) (F).

of conjugation, and killing.[15] Microscopic tracking of non-adherent cells over time is challenging, but the monitoring of conjugates formed between two non-adherent cells, for example between lymphocytes and antigen-presenting non-adherent cells, is problematic. We show here the dynamic conjugation-induced killing in multiple individual conjugates formed between CTLs and cognate target cells held at given positions on a CKChip.

BALB/c mice were immunized against leukemia EL4 cells of C57BL/6 mice by injecting 25×10^6 tumor cells into their peritoneal cavities. This resulted in a complete rejection of the allogeneic tumor 8–10 days later, and generated powerful peritoneal exudate cytocidal CTLs (PELs).[13] CTLs were isolated as described before,[13] stained with a permeable Hoechst dye (nuclear staining, 1 μM), and served as active anti-EL4 CTL. EL4 cells were stained with the viability dye calcein (2 μM). Hoechst stained CTLs and calcein-labeled EL4 cells were co-centrifuged at room temperature for 10 minutes to induce the formation of CTL-EL4 conjugates.[13] Conjugates as well as single CTLs and EL4 target cells were then loaded on the CKChip (Fig. 7A). Temperature-dependent, CTL-mediated killing of conjugated EL4 target cells was recorded by measuring declining cell-bound calcein fluorescence levels (Fig. 7B–E). Non-conjugated EL4 cells served as the internal control. Some of the conjugated target cells were killed rapidly, whereas others were killed more slowly, probably reflecting alternate CTL killing mechanisms.[16]

Discussion

Recent advances in molecular cell biology and medical research are driving a growing need for technologies that enable the examination of dynamic processes in numerous individual living cells over extended periods of time. We have demonstrated here how the CKChip and WELLS dedicated software can be employed to obtain kinetic data from numerous individual, adherent and more importantly non-adherent living cells.

The results underscore the importance of measuring cellular responses at the single-cell level over time, since only then can temporal variability within a population be discerned. We showed considerable heterogeneity in the kinetics of ROS generation following exposure to oxidative stress in H1299 cells (Fig. 4), as previously observed.[17] Since ROS play a critical role in cell signaling, the CKChip provides a new tool for identifying subpopulations of responding cells based on their individual Redox states.

The ability to reveal heterogeneity in the dynamics of individual cells using the CKChip was also demonstrated by measuring the kinetics of enzymatic activity at the single-cell level. Although esterase activity measured in Jurkat cells increased over time, up to a 10 fold variation between cells was observed, probably reflecting the heterogeneity of the population with respect to cell cycle, metabolic activity and other cellular variables[18] (Fig. 5). With the CKChip technology it is now possible to quantify modulation of enzyme activity in numerous individual non-adherent cells.

Simultaneously measuring intracellular Ca^{++} levels and transients in numerous individual cells is important in various research fields, including pharmacology, immunology, neurobiology, cancer, developmental biology and pathology. A number of fluorescence-based methods have been developed to measure alterations in intracellular Ca^{++} levels.[19] Here we showed that addition of DNP-BSA to DNP antibody-sensitized RBL-2H3 cells brought about an increase in fluorescence intensity, followed by sustained oscillations in most cells recorded (Fig. 6A–D). A careful examination revealed wide variations among cells in the amplitude, frequency, time of onset and initial rate of the response. These variations which are of considerable biological significance went undetectable when averaging or when conducting flow cytometry studies (Fig. 6E–F). Oscillations in intracellular calcium following stimulation were previously observed in many cell types[20,21] and numerous studies have focused on their underlying mechanism, and possible consequences.[22] By using the CKChip, it has been possible to follow

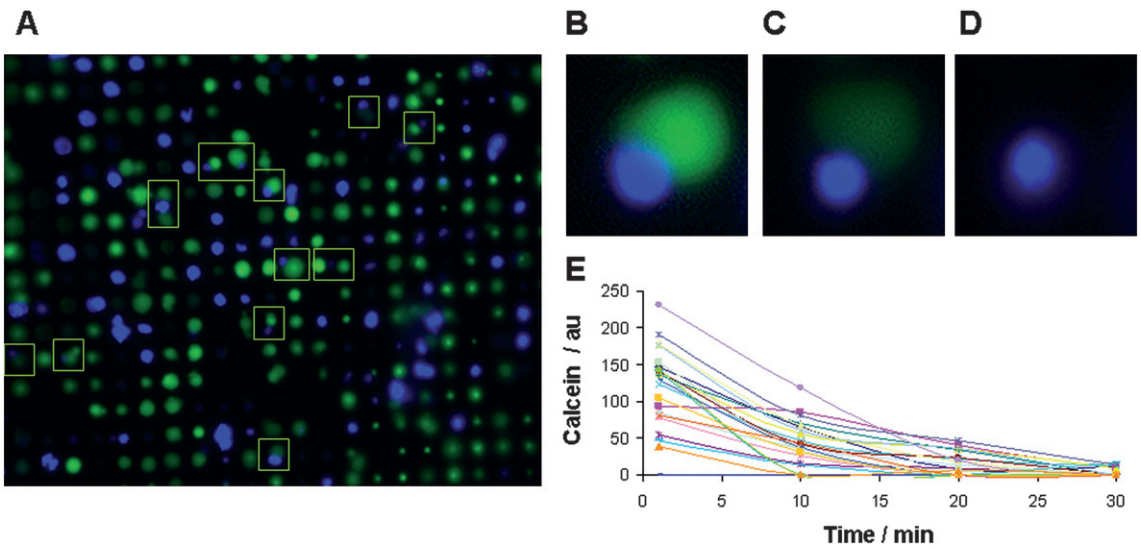

Fig. 7 Kinetics of EL4 target cell killing by conjugated CTLs. EL4 target cells were labeled with calcein (green), and anti-EL4 CTLs were labeled with Hoechst (blue). CTL-EL4 conjugates (some examples squared), as well as single CTLs and EL4 cells were loaded on the CKChip and incubated at 37 °C to induce CTL lytic activity (A). An example of such conjugates revisited 10 (B), 20 (C) and 30 (D) minutes after induction of killing is illustrated. In multiple, distinct bi-cellular conjugates, EL4 killing was assessed by monitoring the loss of calcein fluorescence over time (E).

Ca^{++} oscillations in numerous cells simultaneously, and to determine individual cellular responses over time.

As already stressed, microscopic tracking of temporal events in non-adherent cells over time is challenging, but the monitoring of conjugates formed between two non-adherent cells, for example between lymphocytes and antigen-presenting non-adherent cells, is problematic and requires complex tracking of time-lapse cinematography.[23] The results of the present study confirm the feasibility and convenience of analyzing dynamic cell-cell interactions on the CKChip (Fig 7). Specifically, we have shown the ability to simultaneously monitor target cell killing in hundreds of CTL-target cell conjugates trapped on the CKChip, each conjugate at its specific location ("address"). Ongoing studies address whether the altered killing action of individual CTL plays a role in disease (*i.e.* cancer) and/or drug responses. Other kinetic studies evaluate CTL production and action in vaccination and immunotherapeutic protocols in both basic and clinical laboratory settings.[16]

Traditionally, time-dependent cellular assays with non-adherent cells do not aim at describing single-cell events in heterogeneous cell populations and these are often presented as averages, influenced by wide variations among seemingly identical cells.[1] This is mainly because commonly used cytometric technologies do not enable identification and monitoring of non-adherent cell sub-populations within a mass of cells, over time. Over the last decade different approaches have been developed that enable sequential measurements of individual non-adherent cells allowing gathering kinetic information from many cells at the single-cell level.[2–10] The advantages of the CKChip over existing techniques is, among others, the unique siphoning-based cell loading method involving the use of mild sub-pressure to trap up to 10,000 cells in discrete positions in a fraction of a second. In addition, the embedded code allows for the automatic or manual revisiting of any particular cell of interest among thousands of cells, even after removing the chip from the microscope stage, not requiring the use of sophisticated automatic microscopes. The dedicated WELLS software enables simultaneous, automatic and rapid quantification of different fluorescence-based cell parameters over time in thousands of cells with one click. The CKChip was specially designed for microscopic analysis under low magnifications, allowing kinetic analysis of multiple cells at the single-cell level yielding both valid statistics and identification of rare cell events or behaviour. For this purpose standard microscopes equipped with a rather basic camera are sufficient. When required, high-resolution imaging can be performed, enabling the acquisition of fluorescence-based, high-content kinetic data from multiple, individual non-adherent cells examined on the chip (supplementary material†).

Conclusions

The CKChip enables quantitative, fluorescence-based imaging of numerous cells and their responses to stimuli. Selected cells of interest, both adherent and non-adherent, or groups of cells, can be continuously and simultaneously tracked, measured, manipulated and analyzed a number of times, with their identities verified by their specific location ("addresses") on the chip. The coding system embedded in the chip allows revisiting any cell of interest and by using WELLS dedicated software, various characteristics of thousands of individual living cells, including the kinetics of their responses to stimuli, can be discerned and analyzed. The now commercially available CKChip-system facilitates the simultaneous acquisition of kinetic data from thousands of non-adherent cells within a population of cells.

Supported by grants (to G.B.) received from the Israel Science Foundation and the Kirk Foundation.

References

1 J. L. Spudich and D. E. Koshland Jr., Non-genetic individuality: chance in the single cell, *Nature*, 1976, **262**, 467–71.
2 D. Di Carlo and L. P. Lee, Dynamic single-cell analysis for quantitative biology, *Anal. Chem.*, 2006, **78**, 7918–25.
3 T. C. Chao and A. Ros, Microfluidic single cell analysis of intracellular compounds, *J. R. Soc. Interface*, 2008, **2**, S139–50.
4 A. R. Wheeler, W. R. Throndset, R. J. Whelan, A. M. Leach, R. N. Zare, Y. H. Liao, K. Farrell, I. D. Manger and A. Daridon, Microfluidic device for single-cell analysis, *Anal. Chem.*, 2003, **75**, 3581–3586.
5 M. Deutsch, A. Deutsch, O. Shirihai, I. Hurevich, E. Afrimzon, Y. Shafran and N. Zurgil, A novel miniature cell retainer for correlative high-content analysis of individual untethered non-adherent cells, *Lab Chip*, 2006, **6**, 995–1000.
6 S. Yamamura, H. Kishi, Y. Tokimitsu, S. Kondo, R. Honda, M. Sathuluri Ramachandra Rao, M. Omori, E. Tamiya and A. Muraguchi, Single-Cell Microarray for Analyzing Cellular Response, *Anal. Chem.*, 2005, **77**, 8050–8056.
7 Y. Wakamoto, I. Inoue, H. Moriguchi and K. Yasuda, Analysis of single-cell differences by use of an on-chip microculture system and optical tweezers, *Fresenius J. Anal. Chem.*, 2001, **371**, 276–281.
8 J. R. Retting and A. Folch, Large-scale single-cell trapping and imaging using microwell arrays, *Anal. Chem.*, 2005, **77**, 5628–5634.
9 J. Voldman, M. L. Gray, M. Toner and M. A. Schmidt, A microfabrication-based dynamic array cytometer, *Anal. Chem.*, 2002, **74**, 3984–3990.
10 D. Di Carlo, L. Y. Wu and L. P. Lee, Dynamic single cell culture array, *Lab Chip*, 2006, **6**, 1445–1449.
11 B. Rotman and B. W. Papermaster, Membrane properties of living mammalian cells as studied by enzymatic hydrolysis of fluorogenic esters, *Proc. Natl. Acad. Sci. U S A.*, 1966, **55**, 134–141.
12 D. E. Clapham, Calcium signaling, *Cell*, 2007, **6**, 1047–1058.
13 G. Berke and D. Gabison, Energy requirements of the binding and lytic steps of T-lymphocyte-mediated cytolysis of leukemic cells *in vitro*, *Eur. J. of Immun.*, 1975, **5**, 671–675.
14 G. Berke and W. Clark. In: *Killer Lymphocytes*. Springer Berlin, 2005.
15 G. Berke, The CTL's kiss of death, *Cell*, 1995, **81**, 9–12.
16 O. Gal, Y. S. Schiffenbauer, A. Meiraz and G. Berke. Distinct temporal patterns of lymphocyte action revealed with a new cytomeric platform for simultaneous analysis of numerous lymphocyte (both CD4 and CD8)-target cell conjugates, unpublished work.
17 N. Zurgil, Y. Shafran, E. Afrimzon, D. Fixler, A. Shainberg and M. Deutsch, Concomitant real-time monitoring of intracellular reactive oxygen species and mitochondrial membrane potential in individual living promonocytic cells, *J. Immunol. Methods*, 2006, **316**, 27–41.
18 D. Di Carlo, N. Aghdam and L. P. Lee, Single-cell enzyme concentrations, kinetics, and inhibition analysis using high density hydrodynamic cell isolation arrays, *Anal. Chem.*, 2006, **78**, 4925–30.
19 A. Takahashi, P. Camacho, J. D. Lachleiter and B. Herman, Measurement of intracellular calcium, *Physiol. Rev.*, 1999, **79**, 1089–1125.
20 E. Donnadieu, D. Cefai, Y. P. Tan, G. Paresys, G. Bismuto and A. Trautmann, Imaging early steps of human T cell activation by antigen-presenting cells, *J. Immunol.*, 1992, **148**, 2643–53.
21 P. J. Millard, T. A. Ryan, W. W. Webb and C. Fewtrell, Immunoglobulin E receptor cross-linking induces oscillations in intracellular free ionized calcium in individual tumor mast cells, *J. Biol. Chem.*, 1989, **264**, 19730–39.
22 R. S. Lewis, Calcium oscillations in T-cells: mechanisms and consequences for gene expression, *Biochem. Soc. Trans.*, 2003, **33**, 311–321.
23 D. Zagury, J. Bernard, N. Thierness, M. Feldman and G. Berke, Isolation and characterization of individual functionally reactive cytotoxic T lymphocytes. Conjugation, killing and recycling at the single cell level, *Eur. J. Immunol.*, 1975, **5**, 818–822.

